

Investigation of Optically Grey Electron Cyclotron Harmonics in Wendelstein 7-X

*Neha Chaudhary**, *Johan W. Oosterbeek*, *Matthias Hirsch*, *Udo Höfel*, *Robert C. Wolf*, and *W7-X Team*

Max-Planck-Institut für Plasmaphysik, 17491 Greifswald, Germany

Abstract. For a magnetic field of 2.5T, the electron cyclotron harmonics are spectrally well separated in W7-X as it has a large aspect ratio. Because of this advantage from the geometry of W7-X stellarator, it is easier to scan these higher harmonics (70,140,210.....GHz) compared to tokamaks with small aspect ratio. For confinement reasons, W7-X is planned to work at high plasma densities applying O2 electron cyclotron resonance heating (ECRH). For such plasmas, which already have been demonstrated in experimental campaign OP1.2a of W7-X, electron cyclotron emission (ECE) from second harmonic extraordinary mode (X2) is in cutoff. In that case, optically grey higher harmonics provide the only access to ECE signal and hence electron temperature profiles. A Michelson interferometer will be used in the next operational campaign of W7-X for broadband (50-500 GHz) ECE scan and that will be compared to modeling of ECE emission at different plasma parameters from radiation transport calculations (TRAVIS). The strong stray radiation from non-absorbed ECRH is a major concern in scanning these higher harmonics using an interferometer because this stray radiation will dominate the spectra thus masking the ECE signal. For this purpose, a multimode notch filter design based on a multilayer dielectric structure is constructed to attenuate the stray radiation at 140GHz by 50dB.

1 Introduction

In W7-X for various plasma conditions, the X2 mode of ECE is optically thick and hence it can be taken as a blackbody emission representing an electron temperature [1]. At present, the X2 mode is scanned using a heterodyne radiometer [2] consisting of 32 channels distributed over a frequency range of 120-160 GHz. In OP 1.2a of W7-X, the X2 mode was in cut-off at a plasma density of $1.2 \times 10^{20} \text{ m}^{-3}$ [3]. This demonstrates that there is no direct access to X mode of ECE using the radiometer at high plasma densities. W7-X achieved the highest triple product ($0.68 \times 10^{20} \text{ keVm}^{-3}\text{s}$) [4] for stellarators in OP1.2a. And it is further intended to work at high plasma density considering different modes of electron cyclotron resonance heating [4]. In such scenarios, ECE from optically grey higher harmonics has the potential to be used as the diagnostic tool to get the electron temperature profiles in magnetic confinement devices. To explore diagnostic capability, a Michelson Interferometer [5] will be used to scan these harmonics over a broadband (50-500 GHz) in the next operational campaign OP1.2b of the W7-X. The current work focuses on how to tackle the problem of stray radiation [6] from multiple reflections of non-absorbed ECRH at 140 GHz in the W7-X. A similar situation occurs while scanning the ECE from the radiometer. A Bragg notch filter [2] with notch bandwidth of several 100 MHz is being used to attenuate this stray radiation by approximately 40 dB. However, a monomode Bragg notch filter integrated into a waveguide can be used only for a limited frequency range as it will

introduce notches at extra frequencies as well and will not work for the broad spectral range of Michelson interferometer. Therefore, a multimode notch filter is designed based on a multiple-layer dielectric structure [7] with dielectric layers of high and low refractive indices. The design and corresponding transmission characteristics of the filter are given in following sections.

2 Michelson Interferometer as an ECE diagnostic

A Michelson interferometer will scan the broad spectral range of electron cyclotron harmonics emitted in the W7-X. It is planned to do a cross-calibration of the interferometer with the standard ECE radiometer diagnostic alongside an independent calibration with the hot source. The Michelson Interferometer has a temporal resolution of 23 ms and a spectral resolution of approximately 11 GHz corresponding to mechanically limited mirror excursion of 15mm. The Fourier transform of interferograms will provide the spectral information of ECE. These spectra consisting of higher harmonics of ECE will be explored as an option to get the electron temperature profiles. For further analysis, it is necessary to calculate the broadband ECE spectra from TRAVIS [8]. Hence, one can model electron temperature profiles and plasma density profiles from the microwave radiation transport code TRAVIS. An example from TRAVIS calculations showing higher harmonics of X and O mode ECE with X2 mode in cut-off is given below in Fig. 1.

* Corresponding author: neha.chaudhary@ipp.mpg.de

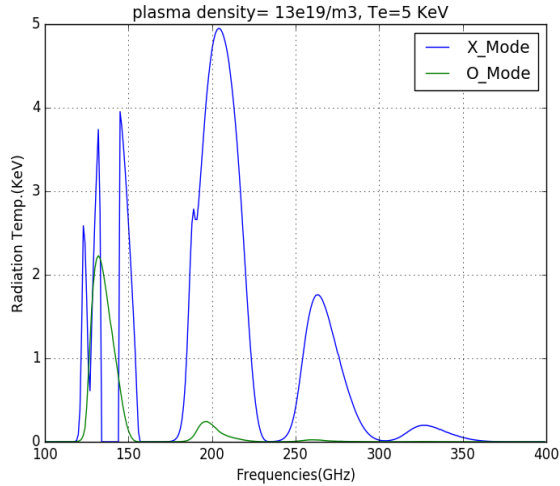


FIG. 1. Higher harmonics of ECE calculated from TRAVIS with parabolic electron temperature and plasma density profiles as input parameters

3 Multimode Notch Filter

Notch filters are generally designed for single cavity applications and for the narrow operational spectral range. Strong stray radiation from non-absorbed ECRH will enter the X2 mode of ECE and it will dominate the ECE in spectra scanned using the interferometer. For this specific application, a notch filter is required for a narrow band stop at 140 GHz to attenuate this stray radiation. Consequently, ECE spectral features will be well defined with the filter.

3.1. Design and transmission of the filter

The design of the filter consists of the structure made up of multiple layers of dielectric with different permittivity. For microwave applications with wavelength (λ) in millimeter range, dielectric plates with thickness of the order of λ can be directly assembled together to construct the filter.

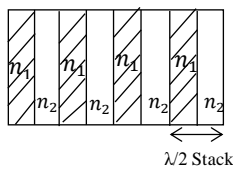


FIG. 2. Schematic of the multimode notch filter with a multilayer structure

The design proposed here for multimode notch filter is consisting of ‘ x ’ number of stacks where one stack is made up of two $\lambda/4$ thick dielectric plates with the refractive indices n_1 and n_2 respectively resulting in a $\lambda/2$ stack as shown in Fig. 2. Transverse reflection coefficients ρ_i for such a structure with $2x + 1$ number of interfaces are given by,

$$\rho_{Ti} = \frac{n_{i-1} - n_i}{n_{i-1} + n_i}, \quad i = 1, 2, \dots, 2x + 1$$

The transmission of this $\lambda/2$ stack structure vanishes at odd multiples of frequency (f) corresponding to λ [7]. The theoretical transmission spectrum of the filter for normal incidence as a function of frequency normalized to 140 GHz is given below,

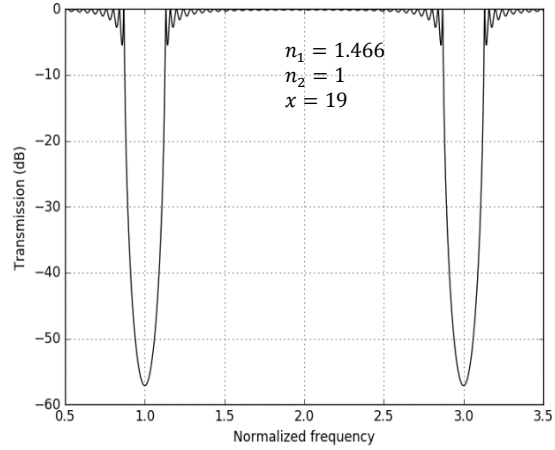


FIG. 3. Theoretical transmission spectrum of the multimode filter

From the theoretical study of the transmission characteristics of such a structure, it is evident that the total number of plates has a direct effect on attenuation at the notch frequency. Hence, depending on the magnitude of attenuation required at the notch frequency one can adjust this parameter accordingly.

3.2 Effect of design parameters on transmission characteristics

3.2.1 Dielectric constant and number of plates

The first transmission minimum in filter characteristic in Fig. 3 is defined as the notch of the filter with corresponding frequency as notch frequency and attenuation in transmission as notch depth. The transmission characteristics of such a structure depend on various physical parameters of the filter such as refractive indices, the thickness of plates, the total number of stacks and angle of incidence θ . The relationship between notch bandwidth Δf and these parameters is given by [7],

$$\frac{\Delta f}{f} = \frac{1}{45} \left[\sin^{-1} \left| \frac{n_1 - n_2}{n_1 + n_2} \right| \text{degrees} \right]$$

For the specific purpose of attenuating stray radiation from nonabsorbed ECRH, a large ratio of notch depth to width is required. This can be achieved by having high refractive indices of two dielectric plates in the stack. Also, the notch depth is directly proportional to the total number of $\lambda/2$ stacks assembled together in filter design as shown in Fig.4.

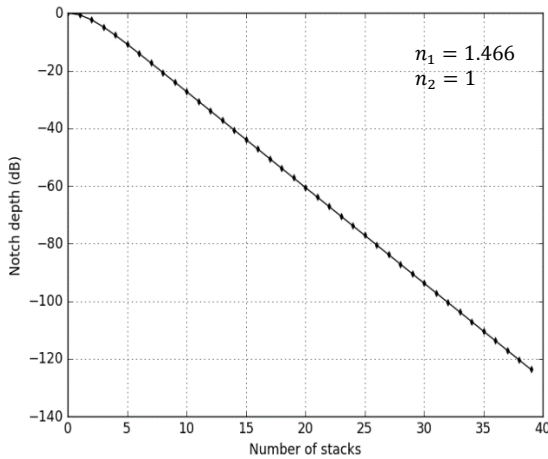


FIG. 4. Variation of notch depth as a function of the total number of stacks

3.2.2 Oblique angle of incidence

For oblique incidence, optical path length traveled by incident rays is equal to optical path length for normal incidence multiplied by the cosine of the angle of transmittance. Depending on the polarization of the incident field, the refractive index has to be replaced by a function of the angle of incidence using Fresnel formula in the calculations [7]. Notch frequency for oblique incidence shifts towards the higher values. This property of the filter can be used in fine-tuning of the notch frequency. Also a small variation in thickness (d_1 and d_2) of either of the plates in the stack can lead to a shift in the notch frequency as shown in Fig. 5.

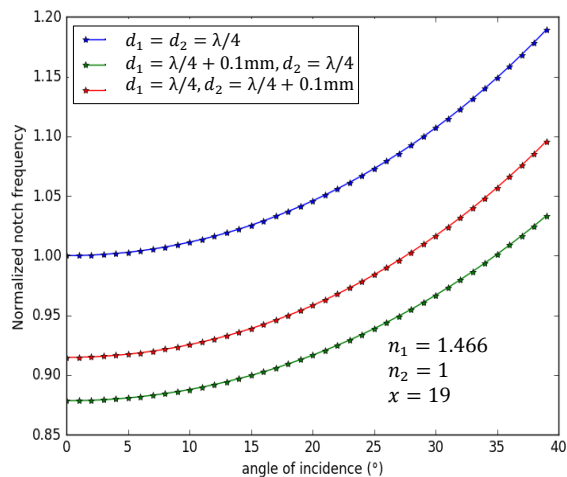


FIG. 5. Notch frequency variation with angle of incidence and thickness of dielectric plates

From the above-shown plot, it can be observed that notch frequency has a strong response to a small variation (0.1 mm) in the thickness of plates.

3.3 Experimental results

A first prototype design test was done with easily available material PTFE which also has low insertion loss

[9]. The stack elements for the filter were PTFE (2.1mm thick) and air gap (2.9mm) introduced by square metal rings (12×12 cm) resulting in one $5\lambda/2$ stack with λ corresponding to 2.32mm and 10 of such $5\lambda/2$ stacks were assembled together to construct the filter. The experimental transmission characteristic of this filter was in good agreement with the theoretical prediction. This led to design the final filter, which will be used with the Michelson to attenuate the stray radiation at 140 GHz. The final filter was constructed with a $3\lambda/2$ stack with λ corresponding to 2.2mm with each stack consisting of PTFE (1.1mm thick) and air-gap (1.65mm). The thicknesses of dielectric plates are chosen to be $3\lambda/4$ instead of $\lambda/4$ because of manufacturing limitations. The circular cross-section in metal rings for introducing air gap was optimized for the input of the Michelson. PTFE and air were chosen as stack elements because they have a small value of $n_1 - n_2$ satisfying the theoretical condition for small Δf . The total number of plates were chosen from the studies of stray radiation at the location of Michelson interferometer [6]. The theoretical broadband transmission spectrum of such a filter design can be calculated easily and it has four notches at odd multiples of $f/3$ in the spectral range of 50-500 GHz. The experimental setup as shown in Fig.6 consisted of a broadband source (120-160 GHz) as input, tapers, and a network analyzer to process the output. Spherical mirrors were used to make input beam parallel with beam waist equal to half of the filter's input cross-section. A rotating platform (optimized for the filter dimensions) was used for the fine-tuning by varying angle of incidences.

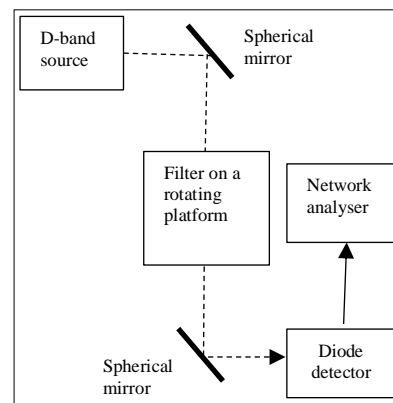


FIG. 6. Schematic of experimental setup

The filter was designed to have notch at slightly lower frequency than 140 GHz and later tune it to 140 GHz by changing the angle of incidence (rotating the filter). This design specificity has an additional advantage other than the tuning of frequency that the reflected power at 140 GHz will not re-enter the input transmission line to the Michelson thus preventing the multiple reflections. The experimental transmission of filter as shown in Fig.7 gives that at 40° with respect to normal incidence there is a 4 GHz wide notch with attenuation of approximately 50dB at 140 GHz.

Experimentally, the notch frequency shifts with a change in the angle of incidence (aoi) as predicted by theory. The experimental results in the frequency range (120-

160GHz) agree with the predicted results. Due to laboratory limitations, the filter was not tested for higher frequency ranges.

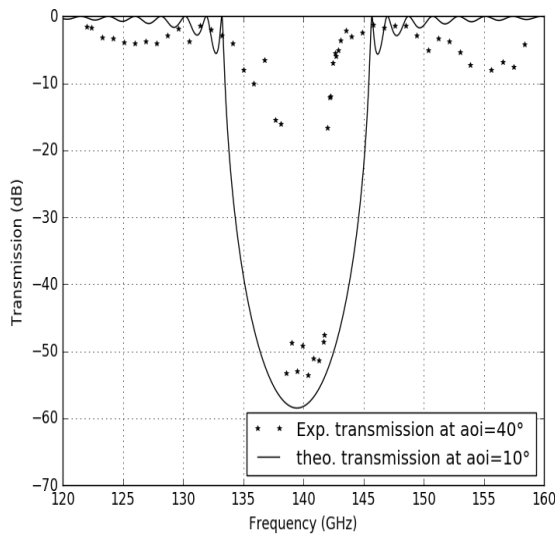


FIG. 7. Experimental transmission characteristics of the notch filter

4 Discussions

Theoretically, a predicted shift in the notch frequency was observed with the change in angle of incidence. But the notch at 140 GHz was predicted at an angle of incidence of 10° opposed to what is observed experimentally at 40° . The explanation for this could be that one 1.1mm thick PTFE plate was assembled by putting 1mm and 0.1mm thick PTFE plates together. The same process was used to create 1.65mm wide air gap by assembling metal rings of 1.5, 0.1 and 0.05mm together. This could have led to a change in the total optical thickness of the structure. Hence, we see the notch frequency of 140 GHz at a higher angle of incidence.

The experimentally observed notch width is smaller compared to the predicted one -- this could suggest that there are further multiple reflections in the structure that we do not understand. The insertion loss at the theoretically transparent part of transmission spectrum is relatively high and hence a proper calibration of the filter will be required at these frequencies.

5 Acknowledgment

This work has been carried out within the framework of the EUROfusion Consortium and has received funding from the Euratom research and training programme 2014-2018 under grant agreement No 633053. The views and opinions expressed herein do not necessarily reflect those of the European Commission.

6. References

- [1] Hartfuss Hans-Jürgen, Geist Thomas, Fusion Plasma Diagnostics with mm-Waves (Wiley-VCH, 2013).
- [2] Hirsch M. et al., Proceedings of the 20th Joint Workshop on Electron Cyclotron Emission and Electron Cyclotron Resonance heating, May 14-17, 2018, Greifswald, Germany.
- [3] Brunner K J. et al., Proceedings of the 20th Joint Workshop on Electron Cyclotron Emission and Electron Cyclotron Resonance heating, May 14-17, 2018, Greifswald, Germany.
- [4] Wolf R C. et al., Electron-cyclotron-resonance heating in Wendelstein 7-X: A versatile heating and current-drive method and a tool for in-depth physics studies, submitted to Plasma Phys. Control. Fusion 2018.
- [5] Austin M E. et al., Rev. Sci. Instrum. **68**, 480 (1997).
- [6] Oosterbeek W J. et al., Proceedings of the 20th Joint Workshop on Electron Cyclotron Emission and Electron Cyclotron Resonance heating, May 14-17, 2018, Greifswald, Germany.
- [7] Young L. et al., IEEE Transactions On Microwave theory And Techniques VOL. MTT-14, NO.2.
- [8] Maruschenko N B. et al., Computer physics Communications 185(2014)165-176.
- [9] Lamb W J. et al., International Journal of Infrared and Millimeter Waves, December 1996, Volume 17, Issue 12, pp 1997-2034.